PHYSICAL REVIEW A
GENERAL PHYSICS

THIRD SERIES, VOLUME 36, NUMBER 8 OCTOBER 15, 1987

Configuration interaction between doubly and singly excited bound states

T. N. Chang and Rong-Qi Wang
Department of Physics, University of Southern California, Los Angeles, California 90089-0484
(Received 30 April 1987)

We present the results of a theoretical investigation on the configuration interaction between doubly excited $(n_1l_1,n_2l_2)^{1,3}L$ and singly excited $(3snl)^{1,3}L$ bound states *below* the first ionization threshold of atomic ions which are isoelectronic to the magnesium atom. The effect of configuration interaction is studied in terms of (i) the term values correction and (ii) the change in oscillator strengths for transitions involving the neighboring singly excited states due to the presence of an individual doubly excited *perturber*. The *range* and *strength* of each bound doubly excited state in Al II and Si III $^{1,3}S$-$^{1,3}F$ series are examined in detail.

I. INTRODUCTION

One of the most interesting features in the spectra of atomic systems with two electrons outside a closed ^1S core (e.g., alkaline-earth atoms) is the strongly-energy-dependent autoionization structure dominated by a series of doubly excited states which are degenerate in energy with the one-electron ionization background channel *above* the ionization threshold. Physical interpretation of the doubly excited autoionization spectra in terms of the configuration interaction has been the subject of many quantitative and qualitative studies following the theoretical approach developed by Fano.[1,2] For the doubly excited state with energy *below* the ionization threshold of the neutral "two-electron" systems such as the heavier alkaline-earth atoms, strong configuration interaction is known to have "diluted" the isolated doubly excited bound state into a series of singly excited bound states.[3] One of the best-known examples is the mixture of the $(3d4p)^1P$ doubly excited state with the $(4snp)^1P$ series in Ca.[4] For lighter alkaline-earth atoms (e.g., Mg and Be), the configuration interaction between the doubly excited states *near or above* the ionization threshold and the series of singly excited states *below* the threshold is still strong enough to have led to a substantial energy correction for many singly excited states. One such example is the strong influence of the $3pnp$ configuration series to the term values of the $(3snd)^1D$ singly excited series.[5,6] In addition, the oscillator strengths for transitions between states of larger total orbital angular momentum are also strongly affected by the configuration interaction such as the large oscillator strength shift seen among the $(3snd)^1D-(3snf)^1F$ transitions in the neutral Mg atom.[7]

The presence of doubly excited states below the first ionization threshold can also be found along the isoelectronic sequence of lighter two-electron systems. This is due to the increase of nuclear attraction for the two outer electrons in the doubly excited state where the mutual screening between the two excited electrons is less complete when compared with the screening experienced by the outer electron in the singly excited state as Z increases. As the doubly excited states in the continuum for neutral atoms "plunge"[8] into the discrete spectrum of ionic systems, the interaction between doubly and singly excited states may lead to a significant shift in term values and at the same time a noticeable redistribution of the oscillator strengths for transitions between excited states. One such example is the interaction between the $3p3d$ perturber and the $(3snf)^3F$ series in Al II.[9] Other earlier theoretical studies[10–12] were also carried out to assess qualitatively the effect of such interaction with a limited numbers of configurations represented by approximate orbital wave functions for the Mg isoelectronic sequence. As for the term values, a highly elaborate multiconfiguration Hartree-Fock (MCHF) calculation has been performed for selected members of the Mg isoelectronic sequence.[8,13]

In a recent attempt[6,7] to develop an effective theoretical procedure which is capable of dealing with the highly excited states in a two-electron system, we have demonstrated that a straightforward superposition of configuration–wave-functions method could be a simple yet very effective calculational approach in the study of configuration interaction for the alkaline-earth atoms. The relatively modest computational requirement and the simplicity of the numerical procedure in this approach has made it possible to carry out a step-by-step quantitative study of the individual physical effect at each stage of approximation. In this paper we will report the application of this procedure to a detailed quantitative investigation of the interaction between isolated

doubly excited states and the series of singly excited states *below* ionization threshold. In particular, we will examine the shift in term values and the redistribution of oscillator strengths in length and velocity approximations for transitions between excited states of Al II and Si III. We will also discuss the "effective range" of the interaction due to the doubly excited state by examining its influence on the term values of the neighboring singly excited states and the oscillator strengths for transitions between these states.

II. CALCULATIONAL PROCEDURE

A detailed description of the theoretical procedure is outlined in our earlier papers.[6,7,14] In this section we will only briefly summarize some of the important elements of the calculational procedure.

Each energy eigenstate of given total spin S and total orbital angular momentum L is represented by a *multiconfiguration-state wave function* Φ. The state function Φ is constructed by a simple superposition of *configuration wave functions* $\Psi^{SL}_{n_i l_i, n_j l_j}$ corresponding to a two-electron configuration $(n_i l_i, n_j l_j)$ outside a closed ^1S core of $N-2$ electrons, i.e.,

$$\Phi(SLM_S M) = \sum_{n_i l_i, n_j l_j} C^{SL}(n_i l_i, n_j l_j)\Psi^{SLM_S M}_{n_i l_i, n_j l_j}(\mathbf{r}_1, \ldots, \mathbf{r}_N) . \quad (1)$$

The configuration wave function Ψ is given in terms of a linear combination of Slater *determinant wave functions* in the LS coupling. Each of the Slater determinant wave functions is in turn constructed with N one-particle orbital wave functions $u_\alpha(\mathbf{r})$ which is the product of its spatial and spin part, i.e.,

$$u_\alpha(\mathbf{r}_\mu) = \chi_{n_\alpha l_\alpha}(r_\mu) Y_{l_\alpha m_\alpha}(\Omega_\mu)\sigma(m_{s_\alpha}) . \quad (2)$$

In the present calculation, the radial part of the one-particle orbital wave function is calculated by solving the one-particle eigenequation

$$h_l^{\mathrm{HF}}(r)\chi_{nl}(r) = \epsilon_{nl}\chi_{nl}(r) , \quad (3)$$

where h_l^{HF} is the one-electron radial Hartree-Fock Hamiltonian constructed with the Ne-like ^1S frozen Hartree-Fock core of $N-2$ electrons. [The detailed expression of h_l^{HF} is given by Eq. (7) in Ref. 14.]

The energy eigenvalue of each energy eigenstate and its corresponding expansion coefficients C^{SL} in Eq. (1) is calculated by diagonalizing the Hamiltonian matrix constructed with the configuration wave functions Ψ from all configurations included in the multiconfiguration expansion. With the one-particle radial wave function χ defined by Eq. (3), the Hamiltonian matrix takes the form[14]

$$\begin{aligned}
&\langle \Psi^{SL}_{n_i' l_i', n_j' l_j'} | H | \Psi^{SL}_{n_i l_i, n_j l_j} \rangle \\
&= [\delta_{n_i' n_i}\delta_{l_i' l_i}\delta_{n_j' n_j}\delta_{l_j' l_j} + (-1)^{l_i + l_j + L + S}\delta_{n_i' n_j}\delta_{l_i' l_j}\delta_{n_j' n_i}\delta_{l_j' l_i}](E_{\mathrm{core}} + \epsilon_{n_i l_i} + \epsilon_{n_j l_j}) \\
&\quad + (-1)^{l_j' - l_i}\left[\sum_k (-1)^L \begin{Bmatrix} l_i' & l_j' & L \\ l_j & l_i & k \end{Bmatrix} \langle n_i' l_i' n_j' l_j' \| V^k \| n_i l_i n_j l_j \rangle + \sum_k (-1)^S \begin{Bmatrix} l_i' & l_j' & L \\ l_i & l_j & k \end{Bmatrix} \langle n_i' l_i' n_j' l_j' \| V^k \| n_j l_j n_i l_i \rangle \right] ,
\end{aligned} \quad (4)$$

where E_{core} is the total Hartree-Fock energy for the $N-2$ core electrons. Since the value of E_{core} is a constant for all states in the frozen-core approximation, E_{core} can be conveniently excluded from the term value calculation. A factor of $2^{-1/2}$ should be included in the Hamiltonian matrix element for configurations with two equivalent electrons. The detailed expression for the Coulomb interactions in Eq. (4) are given elsewhere.[14,15]

With the state wave function Φ constructed following the procedure outlined above, the oscillator strengths f_{ji} for a transition from an initial state i to a final state j in the dipole length and dipole velocity approximation are given by[7]

$$f_{ji}^{l} = \tfrac{2}{3}\Delta E_{ji}\delta_{S_j S_i}(2L_j + 1)\,|\,F_{ji}\,|^2 \quad (5)$$

and

$$f_{ji}^{v} = \tfrac{2}{3}\Delta E_{ji}^{-1}\delta_{S_j S_i}(2L_j + 1)\,|\,F_{ji}\,|^2 , \quad (6)$$

respectively. For transitions limited to the two electrons outside the frozen core, the transition amplitude F_{ji} is given by

$$F_{ji} = \sum_{\text{all configurations}} C^{S_j L_j}(n_j' l_j', n_j l_j) \times C^{S_i L_i}(n_i' l_i', n_i l_i) D_{ji} , \quad (7)$$

where the dipole transition matrix D_{ji} between configuration $(n_j' l_j', n_j l_j)$ and $(n_i' l_i', n_i l_i)$ can be expressed by

$$\begin{aligned}
D_{ji} &= d(j'j, i'i; L_j L_i) + (-1)^{S_i} d(j'j, ii'; L_j L_i) \\
&\quad + d(jj', ii'; L_j L_i) + (-1)^{S_j} d(jj', i'i; L_j L_i) .
\end{aligned} \quad (8)$$

A factor of $2^{-1/2}$ should be included in D_{ji} for configurations with two equivalent electrons. The dipole matrix d is given by the product of the angular factor ρ

and the one-particle radial integral, i.e.,

$$d(j'j,i'i;L_jL_i)=\delta_{n_jn_i}\delta_{l_jl_i}\rho(l_j'l_jl_i'l_i;L_jL_i) \times\langle\chi_{n_j'l_j'}\mid t\mid\chi_{n_i'l_i'}\rangle\ , \tag{9}$$

where the angular factor ρ is given by

$$\rho(l_1l_2l_3l_4;L'L) =(-1)^{l_1}[(2l_1+1)(2l_3+1)]^{1/2}\begin{bmatrix} l_1 & 1 & l_3\\ 0 & 0 & 0\end{bmatrix} \times\begin{Bmatrix} L & 1 & L'\\ l_1 & l_4 & l_3\end{Bmatrix}\delta_{l_2l_4}\ . \tag{10}$$

The operator t in the one-particle radial integral $\langle\chi_{n'l'}\mid t\mid\chi_{nl}\rangle$ represents the radial part of the position and gradient operators in the length and velocity approximation, respectively. The oscillator strength f_{ji} is positive for the *absorption* when the energy difference ΔE_{ji} (a.u.)$=E_j-E_i$ is positive and it is negative for the *induced emission* when ΔE_{ji} is negative.

The energy corrections due to the core dipole polarization and the dielectronic potential introduced by Bottcher and Dalgarno[16] are also included in the Hamiltonian matrix following the procedure outlined in Ref. 14. In the present calculation, the values for the core dipole polarizabilities α are 0.265 and 0.165 a.u. for Al II and Si III respectively. The fitted cutoff radius r_0 equals 0.799 81a_0 for Al II and 0.683 88a_0 for Si III.

III. RESULTS AND DISCUSSION

Following the procedure described in Sec. II, we have carried out numerical calculations for series of states pertaining to $^{1,3}S$, $^{1,3}P$, $^{1,3}D$, and $^{1,3}F$ symmetries for Al II and Si III. For each symmetry (i.e., for a given pair of S and L values), we have diagonalized the Hamiltonian matrix by including a specific set of selected configurations at each stage of approximation. Some of the configuration sets included in the present calculation are listed in Table I.

The calculated term values for all $^{1,3}S-^{1,3}F$ states of Al II and Si III are shown in Figs. 1–4. The energy spectra shown are all relative with respect to the first ionization threshold given at the extreme right and the lowest energy state of each symmetry in rydberg units given at the extreme left. A tall vertical bar in energy spectra represents either a doubly excited state or a state which is strongly mixed with a doubly excited configuration with a probability density [i.e., $\mid C^{SL}\mid^2$ in Eq. (1)] over 25%. The effect due to the interaction between doubly excited states and a series of singly excited states is clearly illustrated by the change in the calculated energy spectra as more configurations are included in each step of the calculation. More quantitative assessment on the effect of individual interaction will be presented in our subsequent discussion.

With the exception of a few states, our converged theoretical term values are in excellent agreement with the experimental data[17] for all symmetries included in the present study. Our calculated term values are also in close agreement with the MCHF results for the ^3F series[13] and some limited states of ^1P and ^1F symmetries[8] for Si III. The present results are generally in closer agreement with the experimental data than other available theoretical term values from earlier calculations.[9–12]

An agreement of better than 1–5 % is found between our "converged" theoretical length and velocity oscillator strengths for most of the $^{1,3}S$-$^{1,3}P$, $^{1,3}P$-$^{1,3}D$, and $^{1,3}D$-$^{1,3}F$ transitions included in the present study. The

TABLE I. Configurations included in the diagonalization of the Hamiltonian matrix at different stages of approximation for $^{1,3}S$-$^{1,3}F$ states.

^1S	^3S	$^{1,3}P$
(SS1) $3s(3-14)s$	(ST1) $3s(4-14)s$	(P1) $3s(3-14)p$
(SS2) SS1$+3p(3-14)p$	(ST2) ST1$+3p(4-14)p$	(P2) P1$+3p(4-14)s$
(SS3) SS2$+3d(3-14)d$ $+4s(4-14)s$	(ST3) ST2$+3d(4-14)d$	(P3) P1$+3p(3-13)d$
(SS4) SS3 + 113 other configurations	(ST4) ST3 + 104 other configurations	(P4) P2$+3p(3-13)d$
		(P5) P4 + 126 other configurations
^1D	^3D	$^{1,3}F$
(DS1) $3s(3-14)d$	(DT1) $3s(3-14)d$	(F1) $3s(4-14)f$
(DS2) DS1$+3p^2$	(DT2) DT1$+3p4p$	(F2) F1$+3p(3-14)d$
(DS3) DS1$+3p(3-14)p$	(DT3) DT1$+3p(4-14)p$	(F3) F2$+3p(5-14)g$
(DS4) DS3$+3p(4-12)f$ $+3d(3-13)d$	(DT4) DT3 + 132 other configurations	(F4) F3$+3d(4-14)p$ $+3d(4-14)f$
(DS5) DS4$+4s(3-13)d$ $+4p(4-13)p$ $+4d(4-12)d$ $+4p(4-11)f$		(F5) F4 + 110 other configurations
(DS6) DS5 + 78 other configurations		

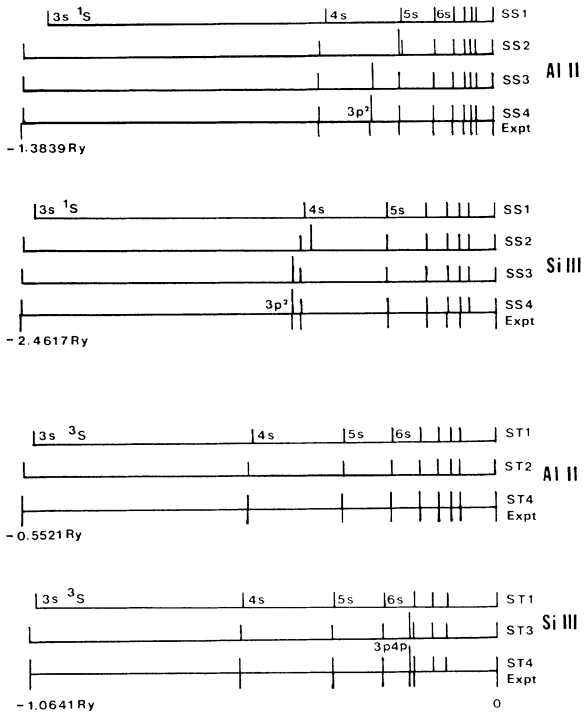

FIG. 1. The $^{1,3}S$ energy spectra of Al II and Si III. The energy in rydberg units is relative to the first ionization threshold at extreme right at zero energy and the lowest energy state of each symmetry on the left at energy shown. Configurations included in each theoretical spectrum are given in Table I. The experimental data are taken from Ref. 17.

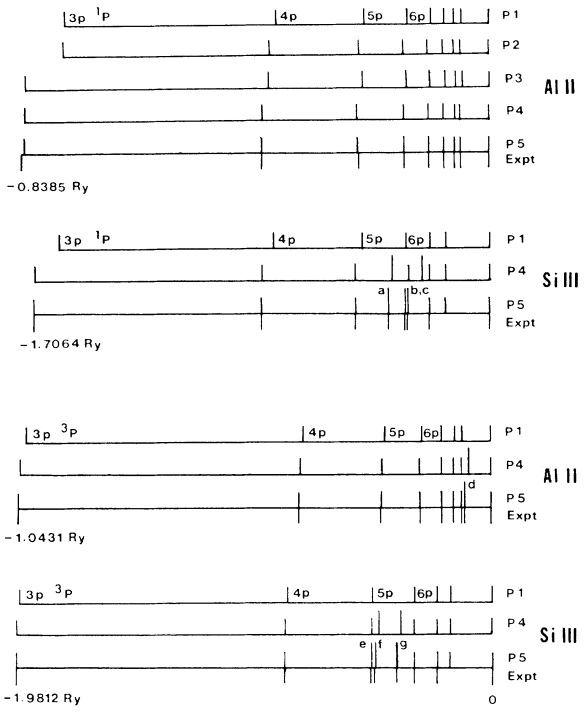

FIG. 2. The $^{1,3}P$ energy spectra of Al II and Si III. The energy in rydberg units is relative to the first ionization threshold at extreme right at zero energy and the lowest energy state of each symmetry on the left at energy shown. Configurations included in each theoretical spectrum are given in Table I. The experimental data are taken from Ref. 17. The states of strong configuration mixing are (a) $3p4s\ ^1P$, (b) $3p3d\ ^1P$, (c) $3s6p\ ^1P$, (d) $3p4s\ ^3P$, (e) $3s5p\ ^3P$, (f) $3p3d\ ^3P$, and (g) $3p4s\ ^3P$.

convergence of the length and velocity results is carefully monitored as we increase the configurations included in the initial and final states of the specific transition. As the main objective of this paper is to examine the effect of the configuration interaction between the discrete doubly and singly excited states below ionization threshold, only limited numerical data on oscillator strengths of few selected transitions involving doubly excited perturber are explicitly listed in Tables II and III. Detailed numerical data will be made available on request.

The interaction between the "plunging" doubly excited states and the series of singly excited states of the same symmetry has been referred to as "strong short-range interaction" by Froese Fischer and Godefroid.[8] The presence of these type of interactions often leads to "local" irregularities in oscillator strengths as Z varies *along the isoelectronic sequence*.[18] In this section we will concentrate our discussion on a *related* but *different* aspect of this interaction, i.e., the "range" and "strength"

TABLE II. Oscillator strengths for selected transitions in Al II involving doubly excited bound states. The top entry represents the length result and the bottom entry represents the velocity result.

n	$(3p^2)^1D$-$(3snf)^1F$	$(3p^2)^1D$-$(3snp)^1P$	$(3sns)^3S$-$(3p4s)^3P$
4	0.348(L)	0.116	0.857
	0.350(V)	0.117	0.841
5	0.122	0.025	0.001
	0.123	0.025	0.001
6	0.060	0.015	0.003
	0.061	0.015	0.003
7	0.035	0.012	0.007
	0.036	0.012	0.007
8	0.023	0.012	0.020
	0.023	0.012	0.021
9	0.016	0.013	0.121
	0.016	0.013	0.123

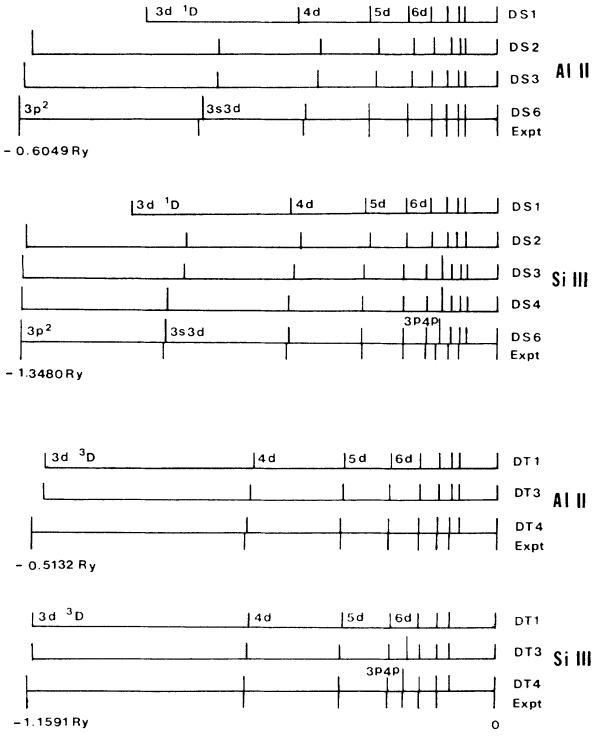

FIG. 3. The $^{1,3}D$ energy spectra of Al II and Si III. The energy in rydberg units is relative to the first ionization threshold at extreme right at zero energy and the lowest energy state of each symmetry on the left at energy shown. Configurations included in each theoretical spectrum are given in Table I. The experimental data are taken from Ref. 17.

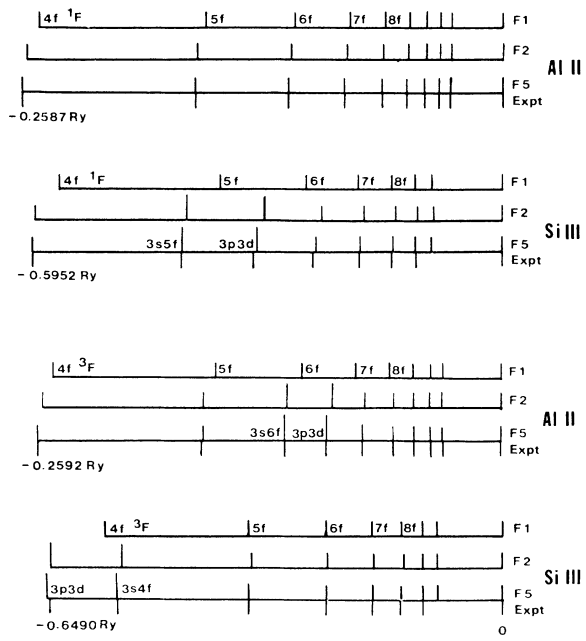

FIG. 4. The $^{1,3}F$ energy spectra of Al II and Si III. The energy in rydberg units is relative to the first ionization threshold at extreme right at zero energy and the lowest energy state of each symmetry on the left at energy shown. Configurations included in each theoretical spectrum are given in Table I. The experimental data are taken from Ref. 17.

of the interaction of an isolated doubly excited perturber *embedded* in a series of singly excited states of the same symmetry in *the same atomic ion.* More specifically, we will examine (i) energy correction of the neighboring singly excited states and (ii) the change of oscillator strengths for transitions involving the neighboring singly excited states due to the presence of the doubly excited perturber. We will consider the strength of the interaction "strong" if a substantial reduction or increase in oscillator strength is experienced by the neighboring singly excited states. The range of the interaction will be measured by the numbers of neighboring states which are affected significantly by the perturber. For example, we will consider the interaction "short-range" if the influence of the perturber is extended only to its immediate neighbors.

A. $3p^2$ in $(3sns)^1S$ series

Figure 1 shows that the $(3p^2)^1S$ state is located between $3s4s$ and $3s5s$ states in Al II and between ground $3s^2$ and $3s4s$ states in Si III. The influence of higher doubly excited $3dnd$ and $4sns$ configuration series above ionization threshold to the term value of the $(3p^2)^1S$ state is evident as the $(3p^2)^1S$ state is pushed away from the $3s5s$ state in Al II and pushed across the $3s4s$ state in Si III. Whereas the term value of the ground $3s^2$ state is clearly affected by the $(3p^2)^1S$ state, the term values for higher ns states are virtually unchanged. This is partly due to the small interaction between $3p^2$ and $3sn(\geq 5)s$ configurations and partly due to the cancellation between corrections from the $3p^2$ and $3pn(\geq 4)p$ configurations.

From the effect on the term values alone, $3p^2$ in ^1S series could easily be classified as a "short-range weak perturber." However, a more detailed examination on the transitions involving $(3sns)^1S$ states will lead us to conclude that the range of the $3p^2$ perturber is not as short as it appears in the term values calculation. Figures 5 and 6 summarize the variation of calculated oscillator strengths in length (dark circle) and velocity (square) approximation for a selected numbers of initial and final state configuration combinations listed in Table I for the ^1S-^1P transitions in Al II and Si III, respectively. Comparison between (SS1,P2) and (SS2,P2) calculations in Fig. 5 for Al II and between (SS1,P1) and (SS2,P1) calculations in Fig. 6 for Si III indicate that the effect of the $3p^2$ perturber on the oscillator strengths for the $(ns)^1S$-$(np)^1P$ transitions is generally small but noticeable and does not diminish significantly as n increases. In fact, the probability density contributions from the $3pnp$ configuration series to $6s$ and $7s$ states for Al II are less than 1% yet the oscillator strength corrections are approximately 10–15 % as shown in Fig. 5.

Interesting variation in oscillator strength is also observed when only some of the configuration series are included in the calculation. One such example is the large increase in oscillator strength from (SS2,P4) to (SS3,P4)

TABLE III. Oscillator strengths for selected transitions in Si III involving doubly excited bound states. Both length (first entry) and velocity (second entry) are listed for each transition. The positive oscillator strength represents an *absorption* and the negative oscillator strength represents an *induced emission*.

	^1D-^1F			^3D-^3F	
$3p^2 \rightarrow 3s4f$	0.456(L)	0.461(V)	$3s6d \rightarrow 3p3d$	−0.021(L)	−0.022(V)
$3p^2 \rightarrow 3s5f$	0.263	0.267	$3p4p \rightarrow 3p3d$	−0.140	−0.144
$3p^2 \rightarrow 3p3d$	0.077	0.078	$3p4p \rightarrow 3s4f$	−0.027	−0.027
$3s3d \rightarrow 3p3d$	0.799	0.802	$3p4p \rightarrow 3s5f$	−0.004	−0.004
$3s4d \rightarrow 3p3d$	0.038	0.040	$3p4p \rightarrow 3s6f$	−0.182	−0.173
$3s5d \rightarrow 3p3d$	0.955	0.931	$3p4p \rightarrow 3s7f$	0.400	0.393
$3s6d \rightarrow 3p3d$	−0.459	−0.436	$3p4p \rightarrow 3s8f$	0.035	0.034
	^1P-^1D			^3P-^3D	
$3s5p \rightarrow 3p^2$	−0.072	−0.072	$3s4p \rightarrow 3p4p$	0.451	0.440
$3p4s \rightarrow 3p^2$	−0.149	−0.147	$3s5p \rightarrow 3p4p$	0.013	0.013
$3p3d \rightarrow 3p^2$	−0.006	−0.006	$3p3d \rightarrow 3p4p$	0.009	0.008
$3s6p \rightarrow 3p^2$	−0.008	−0.008	$3p4s \rightarrow 3p4p$	0.448	0.439
$3s5p \rightarrow 3p4p$	0.002	0.002	$3s6p \rightarrow 3p4p$	0.216	0.206
$3p4s \rightarrow 3p4p$	0.202	0.191			
$3p3d \rightarrow 3p4p$	0.006	0.006			
$3s6p \rightarrow 3p4p$	0.250	0.235			

for the $5s$-$5p$ transition in Al II shown in Fig. 5. The reason for this large difference is due to the "artificially" large mixing between $3p^2$ and $3s5s$ states in the SS2 calculation (see Fig. 1, Al II SS2) when the interaction between $3p^2$ and higher doubly excited configuration series are excluded. As we include the $3dnd$ and $4sns$ configuration series in the SS3 calculation, the $3p^2$ configuration is correctly mixed with the $(3s5s)^1S$ state, and the nearly converged value for the oscillator strength is reached.

For the ground state of Si III, the probability density contribution from $3p^2$ configuration is approximately

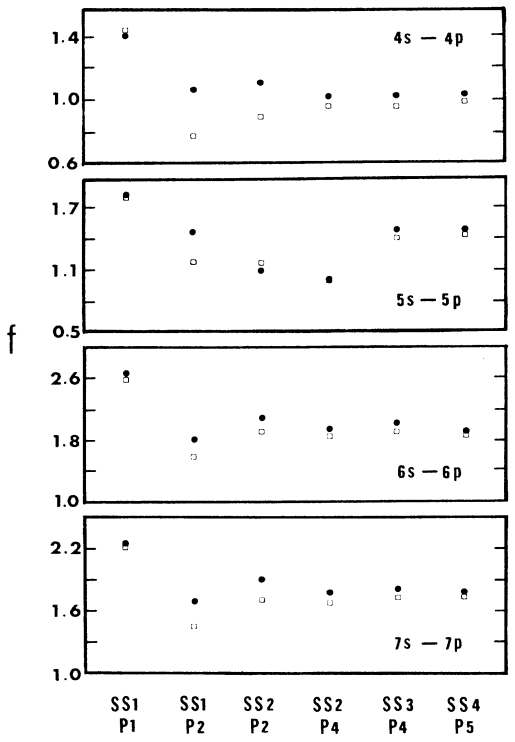

FIG. 5. The calculated oscillator strengths f in length (dark circles) and velocity (squares) approximation for Al II $3sns\ ^1S-3snp\ ^1P$ transitions. The configuration combinations are given in Table I.

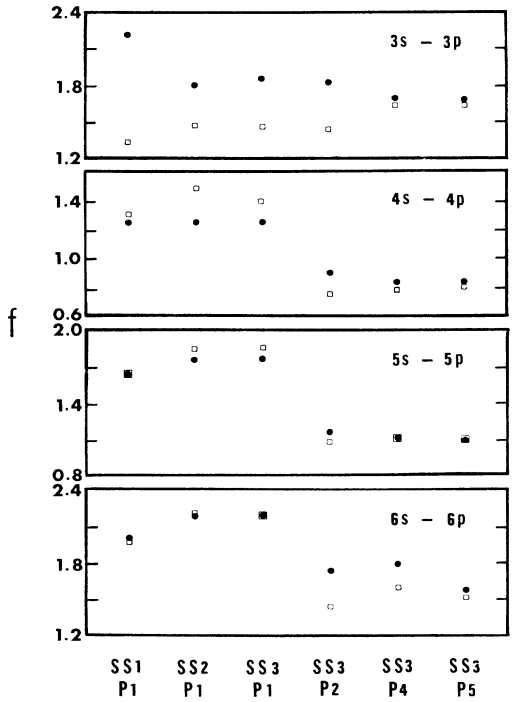

FIG. 6. The calculated oscillator strengths f in length (dark circles) and velocity (squares) approximation for Si III $3sns\ ^1S-3snp\ ^1P$ transitions. The configuration combinations are given in Table I.

4.2% and its effect on the oscillator strength is reflected by the large reduction of the difference between the length and velocity results for the $(3s^2)^1S$-$(3s3p)^1P$ transition shown in Fig. 6 between the (SS1,P1) and (SS2,P1) calculations. Similar corrections are also seen in the $(3s^2)^1S$-$(3s3p)^1P$ transition in Al II (not shown) and Mg.[7] Based on the small but noticeable nondiminishing effect of the $(3p^2)^1S$ state on the oscillator strength for transitions involving many of the $(3sns)^1S$ states, we would classify $3p^2$ in ^1S series as a "medium-range" perturber with "moderate" strength.

B. $3p4p$ in $(3sns)^3S$ series

As shown in Fig. 1, the $(3p4p)^3S$ state in Si III is the only doubly excited state located in the midst of the $(3sns)^3S$ series with energy slightly below but very close to the $(3s8s)^3S$ state. Our calculation has found very little mixing between $3p4p$ and $3sns$ configurations except for the $(3s8s)^3S$ state which has an approximate 10% probability density contribution from $3p4p$. With the exception of the two lowest states in the ^3S series, the term values of all other $(3sns)^3S$ states, including $3s8s$ of Si III, are not affected by the presence of the $3p4p$ configuration. Nor has our calculation found any significant effect on the oscillator strengths for transitions involving states in ^3S series due to the presence of the $(3p4p)^3S$ state. The only noticeable effect is found in the approximate 10% reduction in oscillator strength in the $(3s8s)^3S$-$(3s7p)^3P$ and $(3s8p)^3P$ transitions. We conclude that the $(3p4p)^3S$ state in the $(3sns)^3S$ series is a "highly localized weak perturber."

C. $3p4s$ in $(3snp)^1P$ series

The effects on the term values of the $(3snp)^1P$ states due to the $3p4s$ and its higher members in the $3pn(\geq 5)s$ series are mostly noticeable for $3sn(\geq 4)p$ states. This is clearly demonstrated by the difference between the calculated P1 and P2 spectra of Al II shown in Fig. 2. For Si III, the $(3p4s)^1P$ state is located between the $3s5p$ and $3s6p$ states. Our calculation has shown that the influence due to this perturber and its corresponding configuration series $3pn(\geq 5)s$ on the term values is actually limited only to the $3sn(4-6)p$ states. For $3sn(\geq 7)p$ states, the influence from the $3pn(\geq 4)s$ configuration series is negligible due to the cancellation between opposite corrections from $3p4s$ and $3pn(\geq 5)s$ configurations. The term value correction for the lowest $(3s3p)^1P$ state is primarily due to the $3p3d$ perturber which we will discuss later.

The minimal mixing between the $3p4s$ and $3s3p$ states is also illustrated by the near-zero correction to the oscillator strength for the $3s^2(^1S)$-$3s3p(^1P)$ transition in Si III when comparing the (SS3,P1) and (SS3,P2) calculations shown in Fig. 6. Similar negligible effect is also found in Al II. For $n(\geq 4)p$ states, the oscillator strengths for $(3sns)^1S$-$(3snp)^1P$ transitions are reduced significantly by the presence of the $3p4s$ perturber as shown by the difference between (SS1,P1) and (SS1,P2) calculations for Al II in Fig. 5 and between (SS3,P1) and (SS3,P2) calculations for Si III in Fig. 6. Interestingly but not unexpectedly, this large reduction in oscillator strengths is abruptly diminished as we examine the transitions from the $n=6$ to $n=7$ (not shown) states in Si III. This is expected as we have discussed earlier that the effect due to the $3p4s$ perturber below $3sn(\geq 7)p$ states is canceled by the effect due to higher members in the $3pn(\geq 5)s$ series which are above all $3sn(\geq 7)p$ states. This "short-range" effect is not observed for transitions in Al II where the entire $3pn(\geq 4)s$ series is located above all $3snp$ states included in our calculation.

Similar to what we have observed in the $(3sns)^1S$-$(3snp)^1P$ transitions, the effect of the $3p4s$ perturber and the $3pn(\geq 5)s$ series is of "medium" to "long" range for Al II and "short" to "medium" range for Si III in the ^1P-^1D transitions. This is illustrated by the change in oscillator strength reduction seen between (P1,DS6) and (P2,DS6) in Fig. 7 and between (P1,DS5) and (P2,DS5) in Fig. 8. In spite of the small effect of $3pns$ series to the $(3s^2)^1S$-$(3s3p)^1P$ and $(3s3p)^1P$-$(3s3d)^1D$ transitions, a 30% to over 50% reduction in oscillator strength in many other transitions involving $3snp$ states would make $3p4s$ a moderate to strong perturber for higher $(3snp)^1P$ states.

D. $3p4s$ in $(3snp)^3P$ series

As shown in Fig. 2, the $(3p4s)^3P$ state is located at energy slightly above the $(3s9p)^3P$ state in Al II spectra and between $(3s5p)^3P$ and $(3s6p)^3P$ states in Si III spectra. Our calculation has shown that the term values for all $(3snp)^3P$ series are not affected by the presence of the $3p4s$ perturber with the exception of a small correction for the $(3s9p)^3P$ state in Al II which is located very close to the perturber. The small to negligible difference in the oscillator strength values between (ST1,P3) and (ST1,P4) calculations in Fig. 9 for the ^3S-^3P transitions and between (P3,DT4) and (P4,DT4) calculations in Fig. 10 for the ^3P-^3D transitions in Si III indicate that $3p4s$ is a "highly localized weak perturber" in $(3snp)^3P$ series.

E. $3p3d$ in $(3snp)^1P$ series

A quick examination of our calculated data will immediately lead us to conclude that the $(3p3d)^1P$ state is a localized weak perturber in $(3snp)^1P$ series. For Al II, the $3p3d$ perturber is located above all the $(3snp)^1P$ states included in the present calculation. For Si III, our nonrelativistic calculation has shown that the $3p3d$ perturber is located above the $(3p4s)^1P$ state but nearly degenerate with the $(3s6p)^1P$ state. The noticeable disagreement between the theoretical term value and the observed data can be attributed to the exclusion of the relativistic interaction in the present nonrelativistic LS coupling calculation.[8] A more detailed discussion on the effect of the relativistic interaction will be given in Sec. IV. Our calculation has shown that the effect of the $3p3d$ perturber to the term values of the $3snp$ series is mainly limited to the $(3s3p)^1P$ and $(3s4p)^1P$ states. As for higher members in the $(3snp)^1P$ series, the correction to term value comes primarily from the $3p4s$ perturber as we have discussed earlier.

The influence of the $3p3d$ perturber on transitions in-

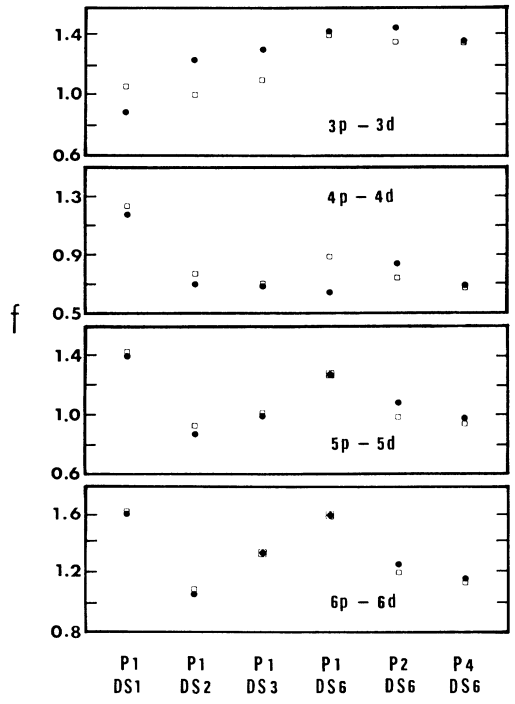

FIG. 7. The calculated oscillator strengths f in length (dark circles) and velocity (squares) approximation for Al II $3snp\ ^1P-3snd\ ^1D$ transitions. The configuration combinations are given in Table I.

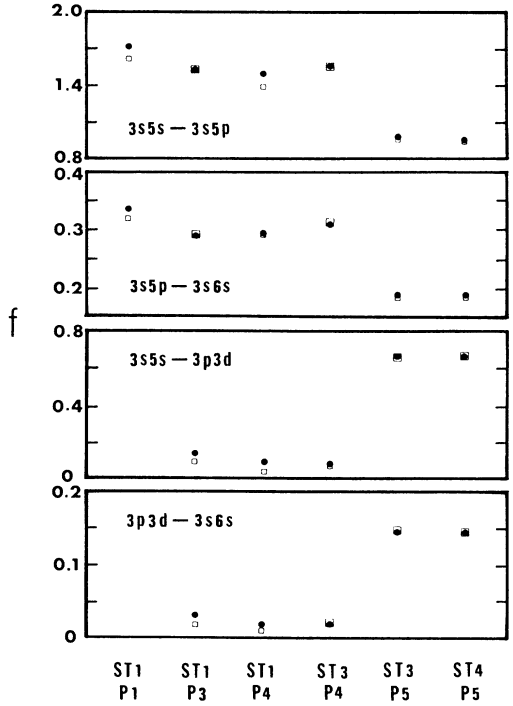

FIG. 9. The calculated oscillator strengths f in length (dark circles) and velocity (squares) approximation for Si III ^3S-^3P transitions. The configuration combinations are given in Table I.

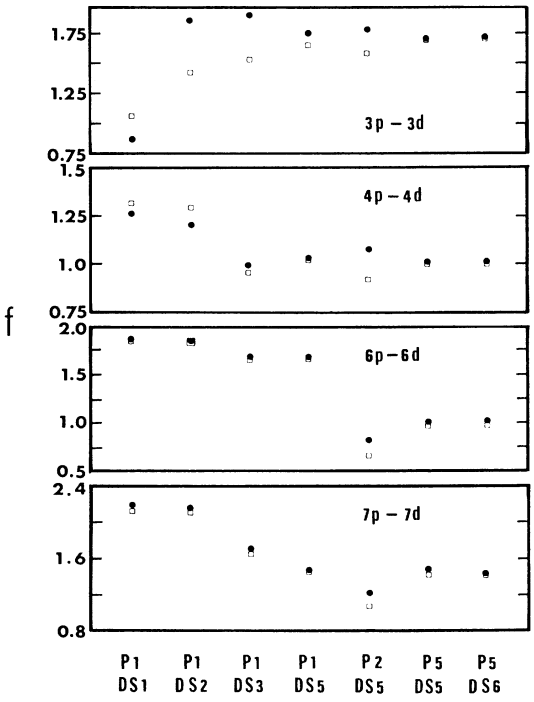

FIG. 8. The calculated oscillator strengths f in length (dark circles) and velocity (squares) approximation for Si III $3snp\ ^1P-3snd\ ^1D$ transitions. The configuration combinations are given in Table I.

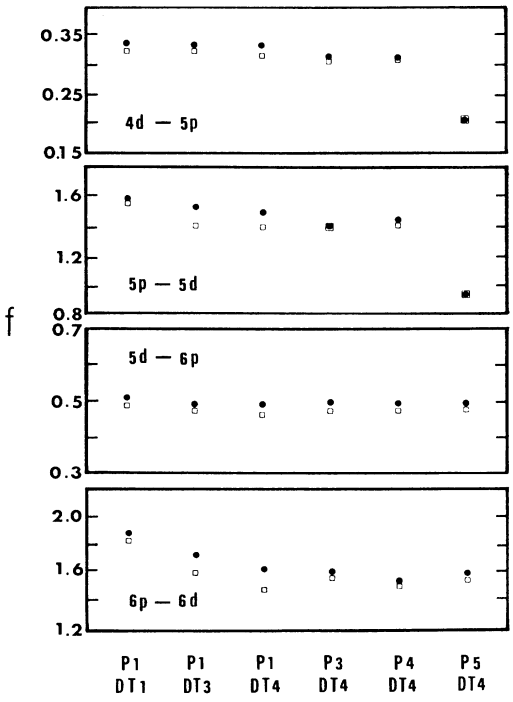

FIG. 10. The calculated oscillator strengths f in length (dark circles) and velocity (squares) approximation for Si III $3snp\ ^3P-3smd\ ^3D$ transitions. The configuration combinations are given in Table I.

volving $(3snp)^1P$ states is generally small as shown by the comparison between (i) (SS2,P2) and (SS2,P4) for ^1S-^1P transitions in Al II in Fig. 5, (ii) (SS3, P2) and (SS3,P4) for ^1S-^1P transitions in Si III in Fig. 6, and (iii) (P2,DS6) and (P4,DS6) for ^1P-^1D transitions in Al II in Fig. 7. The only exception is found in the $(3s^2)^1S$-$(3s3p)^1P$ and $(3s3p)^1P$-$(3s3d)^1D$ transitions where the localized $3p3d$ influence to the $(3s3p)^1P$ state is responsible for the reduction of the difference between length and velocity results as we have shown in Mg (Ref. 7) and also seen in Fig. 6.

F. $3p3d$ in $(3snp)^3P$ series

The $3p3d$ configuration in the $(3snp)^3P$ series could be identified as a highly localized perturber with medium to strong interaction strength. Our calculation has shown that the $(3p3d)^3P$ state of Si III is located slightly above and nearly degenerate with the $(3s5p)^3P$ state. In fact, the probability density contributions to the state labeled as "$3s5p$" are approximately 60% from the $3s5p$ configuration and 39% from the $3p3d$ configuration. For the state labeled as "$3p3d$," the probability density contributions are reversed at approximately 59% from the $3p3d$ configuration, 39% from the $3s5p$ configuration, and 1% from the $3p4s$ configuration. In spite of the strong mixing between $3p3d$ and $3s5p$ configurations in Si III, the term values of the entire $(3snp)^3P$ series are not affected by the $3p3d$ perturber even for the near degenerate "$3s5p$" state as shown in Fig. 2. Similarly, the effect on term values from the $3pnd$ configuration series to the $(3snp)^3P$ series in Al II is also negligible.

Interestingly, our calculation has also shown that the probability density contribution from $3p3d$ to the "$(3s5p)^3P$" state in Si III is only about 5% when the configurations included in the calculation are limited to the $3snp$, $3pns$, and $3pnd$ configuration series (i.e., P4 in Table I). This relatively small mixing is the main reason that only a small change in the oscillator strengths is seen for transitions either started from or ended with the "$(3s5p)^3P$" state. This is shown in Fig. 9 between the (ST1,P1) and (ST1,P3) calculations for the $3s5s$-$3s5p$ and $3s5p$-$3s6s$ transitions and in Fig. 10 between the (P1,DT4) and (P3,DT4) calculations for the ^3P-^3D transitions. As more higher doubly excited configuration series are included in our calculation, the mixing of the $3p3d$ configuration in the "$(3s5p)^3P$" state is increased to 39% as we pointed out earlier; as a result, the oscillator strengths in transitions involving the "$(3s5p)^3P$" state are greatly reduced and at the same time shifted to transitions involving the "$(3p3d)^3P$" state. This is illustrated by the large shift of oscillator strengths between the (ST3,P4) and (ST3,P5) calculations for Si III ^3S-^3P transitions shown in Fig. 9. Similarly, a large reduction of oscillator strengths is experienced in the $(3s4d)^3D$-$(3s5p)^3P$ and $(3s5p)^3P$-$(3s5d)^3D$ transitions as shown in Fig. 10 when we compare the (P4,DT4) and (P5,DT4) calculations. The fact that this shift in oscillator strength is attributed to the short-range interaction due to the $3p3d$ perturber is further confirmed by the nearly constant oscillator strengths between the (P4,DT4) and (P5,DT4) calculations for the neighboring $(3s5d)^3D$-$(3s6p)^3P$ and $(3s6p)^3P$-$(3s6d)^3D$ transitions.

G. $3p^2$ and $3p4p$ in $(3snd)^1D$ series

In neutral Mg the $(3p^2)^1D$ state is known to be the lowest doubly excited state which is located near the first ionization threshold. Therefore, it is not unexpected that it should become the lowest state in the ^1D symmetry for both Al II and Si III as shown in Fig. 3. Our calculation has shown that the mixing between $3p^2$ and $3s3d$ is very strong. In Al II the probability density contribution to the lowest "$(3p^2)^1D$" state is approximately 54% from $3p^2$ and 46% from $3s3d$. The contribution to the next higher "$(3s3d)^1D$" state from the $3p^2$ configuration is approximately 30%. In Si III the contribution to the lowest "$(3p^2)^1D$" is about 67% from $3p^2$ and 32% from $3s3d$ and for the "$(3s3d)^1D$" state is about 70% from $3s3d$ and 29% from $3p^2$. One of the noticeable differences between Al II and Si III is that the mixing from $3p^2$ configuration to other $3snd$ states diminishes rapidly in Si III but not in Al II. In fact, the dominant perturber for the $(3sn(\geq 4)d)^1D$ series in Si III is quickly replaced by the $(3p4p)^1D$ state which is a "diluted state" with a maximum probability density about 40% from the $3p4p$ configuration and located between the $(3s7d)^1D$ and $(3s8d)^1D$ states. The probability density contributions from $3p4p$ to these two neighboring states are approximately 20% and 15%, respectively. This *different assignment* for the $(3p4p)^1D$ state from Ref. 17 is partly suggested by its maximum probability density derived from our calculation and partly supported by the observation that this state is the only state whose energy is corrected significantly when more higher doubly excited configuration series are included as shown by the difference between DS4 and DS6 spectra in Fig. 3. The percentage contribution for all lower states from the present calculation is consistent with other earlier calculations.[12,17]

Similarly to what we have concluded in the case of the neutral Mg atom,[7] the interaction range of the $3p^2$ perturber in Al II $(3snd)^1D$ series is longer than all other perturbers we have examined so far. This is first seen by the noticeable energy difference between calculated Al II energy spectra DS1 and DS2 shown in Fig. 3. From Al II DS3 spectra, we find that for $3sn(\geq 9)d$ states, this energy correction is almost completely canceled by correction due to the higher $3pn(\geq 4)p$ configuration series. For Si III, the difference between the DS1 and DS2 spectra in Fig. 3 suggests that the energy increase of the $3snd$ states due to $3p^2$ configuration is extended only to the $(3s5d)^1D$ state. On the other hand, a negative energy correction is added to all $3sn(\leq 7)d$ states below the $3p4p$ state due to the presence of the $3p4p$ perturber and other higher configuration series as shown by the Si III DS3 and DS4 spectra in Fig. 3.

In spite of the large mixing ($\sim$30%) from the $3p^2$ perturber to the $(3s3d)^1D$ state, only a moderate increase of approximately 15–20% in oscillator strength is seen in the $(3s3p)^1P$-$(3s3d)^1D$ transition in Al II. In contrast, a

relatively small mixing of $3p^2$ perturber in higher $(3snd)^1D$ states in Al II has led to a substantial reduction of the oscillator strengths in the $(3snp)^1P$-$(3snd)^1D$ transitions as shown by the difference between (P1,DS1) and (P1,DS2) calculations in Fig. 7. For higher $(3snd)^1D$ states, this reduction is first partially canceled by a moderate but still significant increase in oscillator strengths due to higher members in the $3pn(\geq 4)p$ configuration series and then almost completely canceled by increase due to other higher configuration series as shown in the (P1,DS3) and (P1,DS6) calculations in Fig. 7.

The influence of the $3p^2$ perturber in Si III is quite different. The fact that $3p^2$ is a short-range perturber in the Si III $(3snd)^1D$ series is also illustrated in the oscillator strength corrections shown by (P1,DS1) and (P1,DS2) calculations for the $(3snp)^1P$-$(3snd)^1D$ transitions in Fig. 8. As expected, the only noticeable correction due to the $3p^2$ perturber is limited to the $3s3p$-$3s3d$ transition. The change of oscillator strengths due to higher $3pn(\geq 4)p$ configurations is generally small for the $(3snp)^1P$-$(3snd)^1D$ transitions except for the $n=7$ transition in that the final $(3s7d)^1D$ state is strongly mixed with the $(3p4p)^1D$ perturber. The only other exception is found in the $3s4p$-$3s4d$ transition. The (P1,DS3) calculation in Fig. 8 shows that the oscillator strengths for these two transitions are reduced significantly. For the $(3s4p)^1P$-$(3s4d)^1D$ transition, this large reduction results primarily from the large correction to the dipole matrix element D_{ji} from the matrix element $\langle 3p \mid t \mid 3s \rangle \langle 4p \mid 4p \rangle$ between the dominant $3s4p$ configuration in the initial state and the non-negligible $3p4p$ component (i.e., $C^{SL} \sim 0.17$) in the final state.

We will now turn our attention to the ^1D-^1F transitions in Al II. With F3 configurations included in the final ^1F state calculation, the effects of the $3p^2, 3pn(\geq 4)p$ configuration series, and other higher configuration series to the $3snd(^1D)$-$3s(n+1)f(^1F)$ transitions are illustrated in Fig. 11 by varying the configurations included in the initial ^1D states from DS1, DS2, DS3, to DS4. Similar to what we have learned in the ^1P-^1D transitions in Al II, the influence of the $3p^2$ perturber *alone* to the ^1D-^1F transitions is significant even for transitions involving higher n states which are only nominally mixed with $3p^2$. This large increase in oscillator strengths for higher n states is mostly canceled by the correction due to the $3pn(\geq 4)p$ configuration series. When more higher configuration series are included in DS4 calculation, the increase in oscillator strengths due to the $3p^2$ perturber is almost completely canceled. The only transition with a significant *net* change in oscillator strength is the $(3s3d)^1D$-$(3s4f)^1F$ transition.

The presence of two doubly excited perturbers, i.e., $3p^2$ and $3p4p$, in the Si III $(3snd)^1D$ series has made a detailed analysis of oscillator strength variation in ^1D-^1F transitions more complicated. In Figs. 12–14 we present the calculated oscillator strengths for the $3snd$-$3snf$, $3snd$-$3s(n+1)f$, and $3snd$-$3s(n+2)f$ transitions.

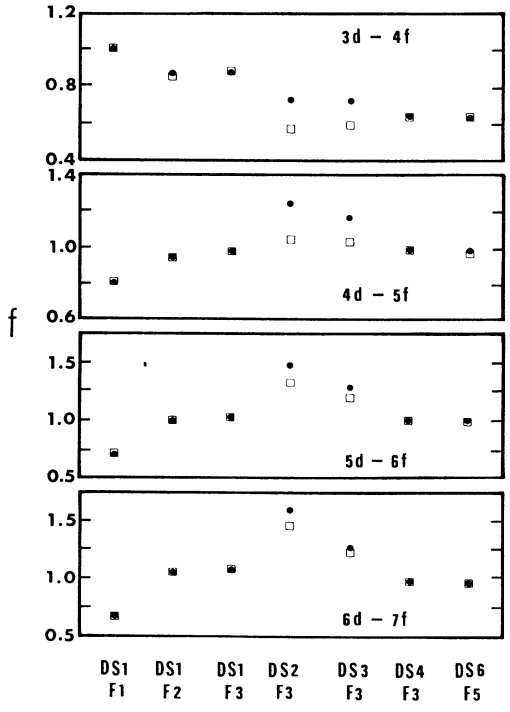

FIG. 11. The calculated oscillator strengths f in length (dark circles) and velocity (squares) approximation for Al II $3snd\ ^1D-3s(n+1)f\ ^1F$ transitions. The configuration combinations are given in Table I.

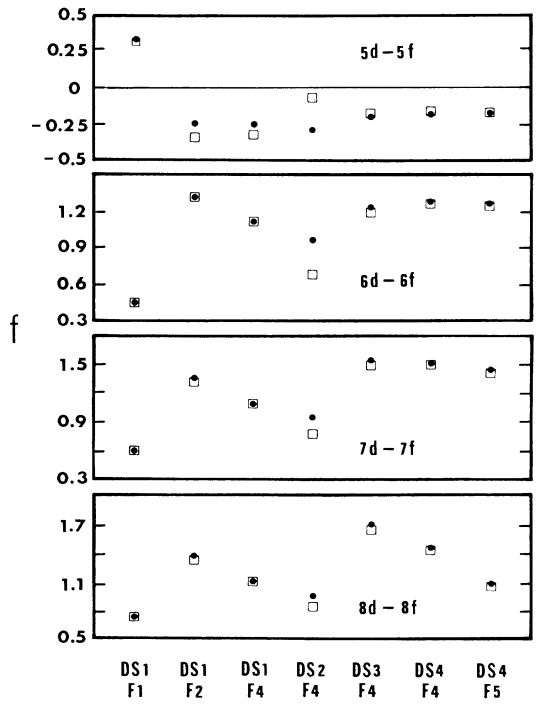

FIG. 12. The calculated oscillator strengths f in length (dark circles) and velocity (squares) approximation for Si III $3snd\ ^1D-3snf\ ^1F$ transitions. The configuration combinations are given in Table I.

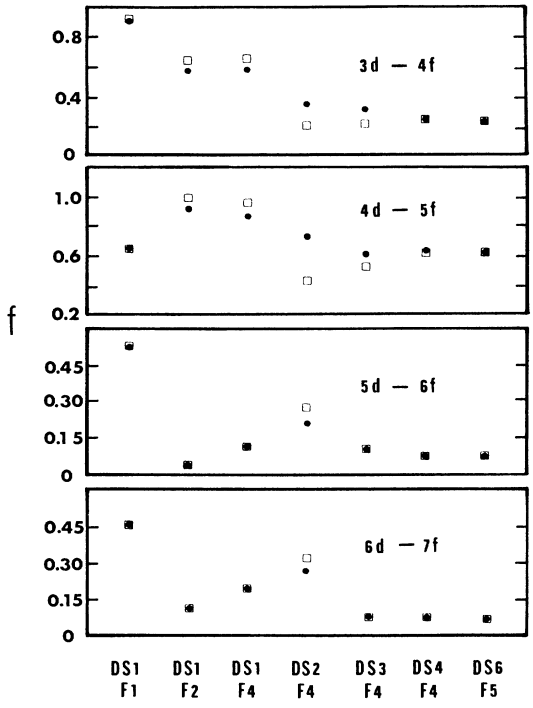

FIG. 13. The calculated oscillator strengths f in length (dark circles) and velocity (squares) approximation for Si III $3snd\ ^1D-3s(n+1)f\ ^1F$ transitions. The configuration combinations are given in Table I.

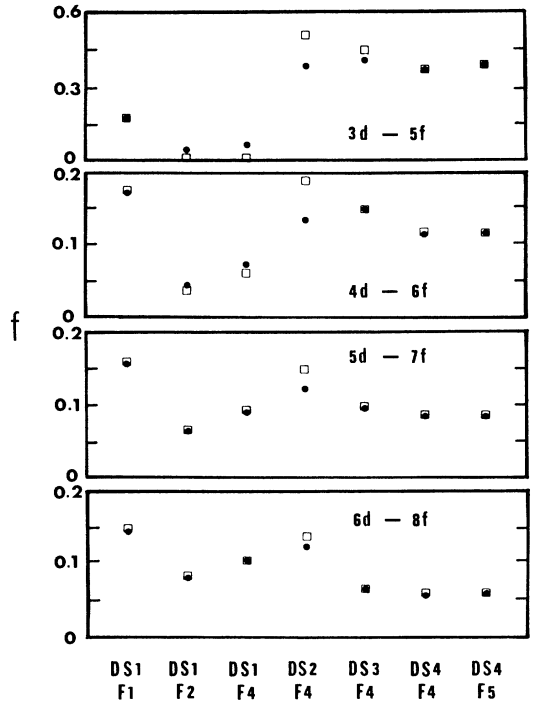

FIG. 14. The calculated oscillator strengths f in length (dark circles) and velocity (squares) approximation for Si III $3snd\ ^1D-3s(n+2)f\ ^1F$ transitions. The configuration combinations are given in Table I.

The effect due to the configuration interaction in the ^1D states of Si III is represented by the variation from (DS1,F4), (DS2,F4), (DS3,F4), to (DS4,F4) calculations. Consistent with what we have learned earlier, the change in oscillator strengths for transitions involving lower $3snd$ states is mostly dominated by the $3p^2$ perturber. The correction due to the $3pn(\geq 4)p$ configurations for transitions of these lower n states is small. On the other hand, for transitions involving higher $3snd$ states, the effect due to the $3p^2$ perturber is generally small and the change in oscillator strengths comes primarily from the effect due to the $3p4p$ perturber. The cancellation between corrections due to different configuration series has made the *net* change in oscillator strengths fairly modest except in the $(3s3d)^1D$-$(3snf)^1F$ transitions.

H. $3p4p$ in $(3snd)^3D$ series

In Al II the $(3p4p)^3D$ state is located above all the $(3snd)^3D$ states included in the present calculation. In Si III the $(3p4p)^3D$ perturber, with a probability density of approximately 75% from the $3p4p$ configuration, is located between the $(3s6d)^3D$ and $(3s7d)^3D$ states. Figure 3 shows that these two immediate neighboring states are the only states whose term value is noticeably affected by the $3p4p$ and higher $3pn(\geq 5)p$ configuration series. As for the oscillator strength, very little change is seen for transitions in Al II due to the effect from the $3pnp$ configuration series. [See, e.g., some of the ^3D-^3F transitions shown in Figs. 15 and 16 between (DT1,F1) and (DT3,F1) calculations.] In Si III our calculation shows that the only transitions that are subject to the influence of the $3p4p$ perturber are those involving either the $(3s6p)^3D$ or the $(3s7d)^3D$ state which are located next to the $(3p4p)^3D$ states. For example, in the ^3P-^3D transition, the comparison between (P1,DT1) and (P1,DT3) calculations in Fig. 10 shows that only in the $3s6p$-$3s6d$ transition is the oscillator strength noticeably changed by the $3pnp$ series. The effect due to the short-range $3p4p$ perturber *alone* could be as drastic as the large reduction in oscillator strength in the $(3s7d)^3D$-$(3s8f)^3F$ transition shown by the (DT1,F5) and (DT2,F5) calculations in Fig. 17. The influence due to higher $3pn(\geq 5)p$ configurations are also illustrated by the (DT3,F5) calculation in Fig. 17.

I. $3p3d$ in $(3snf)^1F$ series

Our calculation shows that in Si III the $(3p3d)^1F$ perturber is a *highly* "diluted state" with a *maximum* probability density contribution of approximately 32% from the $3p3d$ configuration located between the "$(3s5f)^1F$" and "$(3s6f)^1F$" states as shown in Fig. 4. In fact, the probability density contribution from $3p3d$ for the lower neighboring "$(3s5f)^1F$" is almost as large at approximately 30% which is in agreement with the earlier calculation.[12] For the higher neighboring "$(3s6f)^1F$" state, the contribution from $3p3d$ is smaller at about 11%. For Al II our calculation shows that the $(3p3d)^1F$ state is

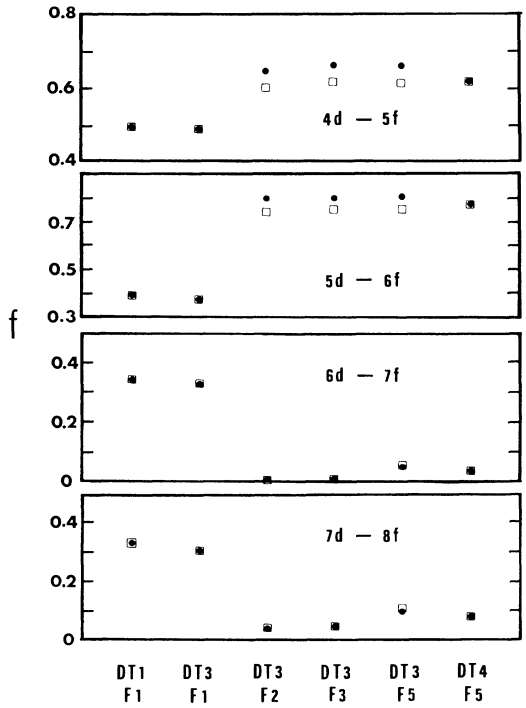

FIG. 15. The calculated oscillator strengths f in length (dark circles) and velocity (squares) approximation for Al II $3snd\ ^3D-3s(n+1)f\ ^3F$ transitions. The configuration combinations are given in Table I.

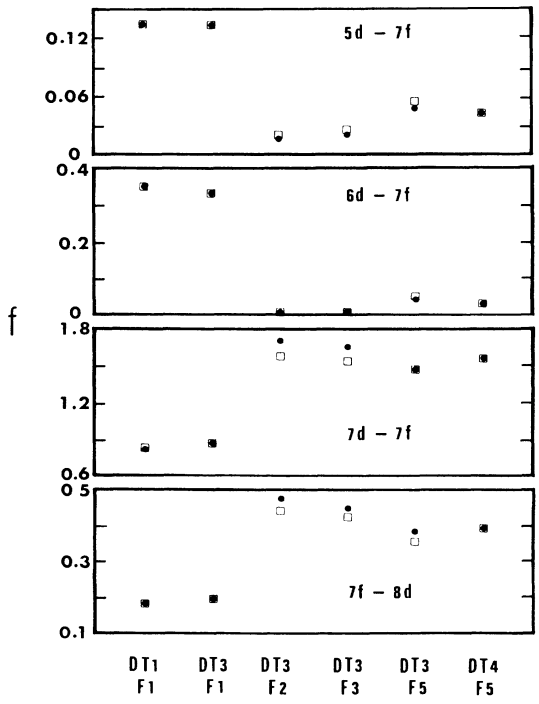

FIG. 16. The calculated oscillator strengths f in length (dark circles) and velocity (squares) approximation for Al II $3snd\ ^3D-3s7f\ ^3F$ transitions. The configuration combinations are given in Table I.

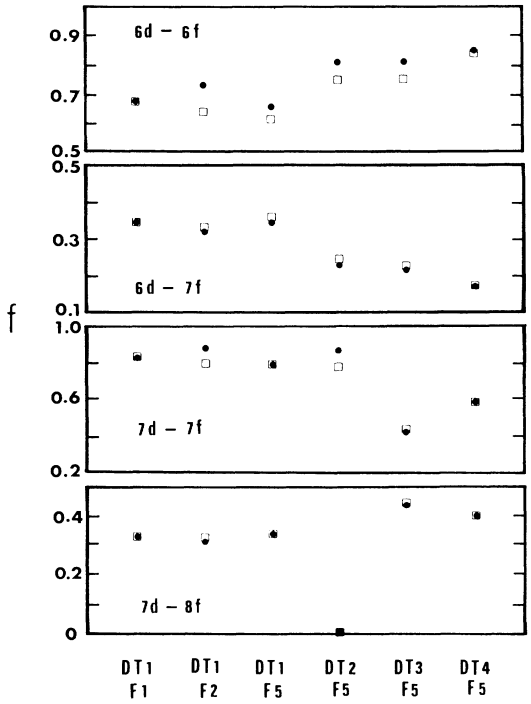

FIG. 17. The calculated oscillator strengths f in length (dark circles) and velocity (squares) approximation for Si III $3snd\ ^3D-3smf\ ^3F$ transitions. The configuration combinations are given in Table I.

located above all the $(3snf)^1F$ states included in the present study.

Although the term value correction for the Al II $(3snf)^1F$ series due to the $3pnd$ configuration series is generally small, Fig. 4 shows that the correction is noticeable to states at least up to $n=10$. In contrast, the term value correction for the Si III $(3snf)^1F$ series is generally larger but its range is extended only to about the $n=8$ state due to the cancellation effect between $3p3d$ and higher $3pnd$ configurations.

Similar to the influence of the $3pn(\geq 4)s$ configuration series to the $(3snp)^1P$ series in Al II discussed in Sec. III C, our calculation shows that the range of the interaction between the $3pnd$ doubly excited configuration series and the $(3snf)^1F$ series in Al II is relatively long and its strength varies from weak to moderate. This is supported by the moderate but persistent oscillator strength increase from (DS1,F1) to (DS1,F2) shown in Fig. 11 for the Al II $3snd(^1D)$-$3s(n+1)f(^1F)$ transitions. In addition, the (DS1,F3) calculation in Fig. 11 shows that the effect due to the higher $3png$ configuration series is practically zero.

For Si III the large mixing of $3p3d$ in the "$(3s5f)^1F$" state has pushed the "$(3s5f)^1F$" state from above to below the $(3s5d)^1D$ state; consequently, the $(3s5d)^1D$ to $(3s5f)^1F$ absorption is changed into $(3s5d)^1D$ to $(3s5f)^1F$ emission. This is illustrated in Fig. 12 between (DS1,F1) and (DS1,F2) calculations where the oscillator strength value changes from positive to negative. Interestingly, we also note that at the same time a substan-

TABLE IV. Oscillator strengths for the *absorption* between $(3snd)^3D$ and $(3snf)^3F$ states in Al II. The length (first entry) and velocity (second entry) values are both listed for each transition. The oscillator strengths for $(3s3d)^3D$-$(3snf)^3F$ transition from Weiss (Ref. 9) are also given (last entry for $3d$-nf transitions) for comparison.

	3d	4d	5d	6d	7d	8d
4f	0.633(L)	0.204	0.023	0.0032	0.001	0.0004
	0.634(V)	0.212	0.024	0.0035	0.001	0.0005
	0.637(Ref. 9)					
5f	0.043	0.617	0.198	0.034	0.005	0.002
	0.043	0.614	0.208	0.035	0.006	0.002
	0.037					
6f	0.0425	0.088	0.772	0.124	0.005	0.001
	0.0414	0.088	0.768	0.119	0.006	0.001
	0.046					
3p3d	0.257	0.008	0.0096	1.211	0.351	0.019
	0.254	0.008	0.0096	1.209	0.353	0.019
	0.251					
7f	0.161	0.045	0.042	0.032	1.537	0.388
	0.160	0.045	0.042	0.031	1.541	0.393
	0.242					
8f	0.0777	0.034	0.041	0.056	0.078	1.630
	0.0776	0.034	0.041	0.056	0.077	1.632
	0.166					
9f	0.044	0.023	0.029	0.039	0.059	0.096
	0.044	0.023	0.029	0.039	0.058	0.095

tial increase in oscillator strength is seen for other $3snd$-$3snf$ transitions between higher n states. In fact, a similar oscillator strength redistribution due to the presence of the $3pnd$ perturbers can also be found between (DS1,F1) and (DS1,F2) calculations in Figs. 13 and 14 for $3snd(^1D)$-$3s(n+1)f(^1F)$ and $3snd(^1D)$-$3s(n+2)f(^1F)$ transitions. The effect due to other higher configuration series is also illustrated by the (DS1,F4) calculations in Figs. 12–14. This large oscillator strength shift seen in ^1D-^1F transitions leads us to conclude that $3p3d$ is a strong perturber of medium range. We also note that from Figs. 13 and 14 our calculation has concluded that the combined effect resulted from the $3p^2$ in the $(3s3d)^1D$ state and the $3p3d$ in the $(3snf)^1F$ series has made $(3s3d)^1D$-$(3s5f)^1F$ a more probable transition than $(3s3d)^1D$-$(3s4f)^1F$.

J. $3p3d$ in $(3snf)^3F$ series

Similar to $3p3d$ in the ^1F series of Si III, the $(3p3d)^3F$ perturber is a "diluted state" in the Al II $(3snf)^3F$ series with a *maximum* probability density contribution of approximately 36% from the $3p3d$ configuration located between the $(3s6f)^3F$ and $(3s7f)^3F$ states as shown in Fig. 4. Our calculation has found that the probability density contributions of these two neighboring states from $3p3d$ are about 28% and 12%, respectively. The mixing percentages from the present calculation are in close agreement with the MCHF calculation[13] but somewhat different from the referred values in Ref. 17 from earlier calculation.[9] Our calculated nonrelativistic term values excluding the J splitting for the Al II ^3F series are generally in very close agreement with the experimental

TABLE V. The *range* and *interaction strength* of the doubly excited perturber to singly excited $(3snl)^{1,3}L$ series in Al II and Si III.

Perturber	Range	Interaction strength
$(3p^2)^1S$	medium	moderate
$(3p4p)^3S$	short	weak
$(3p4s)^1P$	medium–long (Al II)	moderate–strong
	short–medium (Si III)	
$(3p4s)^3P$	short	weak
$(3p3d)^1P$	short	weak
$(3p3d)^3P$	short	moderate–strong
$(3p^2)^1D$	long (Al II)	moderate (Al II)
	short (Si III)	weak–moderate (Si III)
$(3p4p)^3D$	short (Si III)	weak–moderate (Si III)
$(3p3d)^1F$	long (Al II)	weak–moderate (Al II)
	medium (Si III)	strong (Si III)
$(3p3d)^3F$	medium–long (Al II)	strong (Al II)
	short (Si III)	weak (Si III)

data as shown in Fig. 4.

Our calculation has also shown that $3p3d$ is a more localized perturber in the Si III ^3F series with a probability density contribution of about 77% from $3p3d$ configuration. In fact, it is located below all singly excited $(3snf)^3F$ states. The only other states in the ^3F series with non-negligible mixing are the $(3s4f)^3F$ and $(3s5f)^3F$ states with 20% and 1.2% probability density contribution from $3p3d$, respectively. Our calculated mixing percentages are also in close agreement with earlier calculation[12,17] and Fig. 4 shows that the term values for all Si III ^3F states included in the present calculation are in very good agreement with the experimental data.[17]

The redistribution of oscillator strengths due to the mixing of $3p3d$ in the $(3snf)^3F$ series in Al II ^3D-^3F transitions was first investigated quantitatively by Weiss.[9] Our present calculation shows that the redistribution of oscillator strength is not just limited to the $(3s3d)^3D$-$(3snf)^3F$ transitions. In Figs. 15 and 16 we present some of the transitions involving higher n states which are strongly affected by the $3p3d$ perturber. We will first concentrate on the unusually large shift in oscillator strength between (DT3,F1) and (DT3,F2) calculations. In particular, we note in Fig. 16 that this large change in oscillator strength is clearly associated with the $(3s7f)^3F$ state which is the immediate neighbor on the higher energy side of the $(3p3d)^3F$ perturber. As we move away from the $(3p3d)^3F$ perturber, the change in oscillator strength becomes less dramatic and gradually reduces to a more modest increase such as the one seen in the $3s4d$-$3s5f$ transition in Fig. 15. The influence due to other higher configuration series is much smaller as shown by the (DT3,F3) and (DT3,F5) calculations in Figs. 15 and 16. Our calculated oscillator strength distribution for the ^3D-^3F transitions in Al II is qualitatively in agreement with the earlier estimation of Weiss[9] with larger disagreement for transitions involving higher n states as shown in Table IV.

In contrast, in Si III, our calculation shows that the change of oscillator strengths for the ^3D-^3F transitions is generally very small even for transitions involving the lowest $(3s4f)^3F$ state which is strongly mixed with the $3p3d$ perturber. This is partly due to the localized nature of the $3p3d$ perturber and partly due to the cancellation between corrections due to $3p3d$ and higher members in the $3pnd$ configuration series. This minimal effect due to the $3pnd$ series in the Si III ^3D-^3F transitions can be seen from the (DT1,F1), (DT1,F2), and (DT1,F5) calculations shown in Fig. 17.

IV. CONCLUDING REMARKS

Following our discussion in Sec. III, we summarize in Table V the *strength* and *range* of the interaction due to individual doubly excited perturber to series of singly excited $(3snl)^{1,3}L$ states in Al II and Si III. Similar to what we have learned in the neutral Mg atom studies,[6,7] the current work also shows that for transitions between singly excited states of higher total orbital angular momentum, the interaction due to strong doubly excited perturber and in some cases even a moderate perturber could lead to an extensive oscillator strength redistribution. This is illustrated by many of the examples given in Sec. III including (i) ^1P-^1D transitions in Al II (Fig. 7) and Si III (Fig. 8), (ii) Si III ^3S-^3P transitions (Fig. 9), (iii) ^1D-^1F transitions in Al II (Fig. 11) and Si III (Figs. 12–14), and (iv) ^3D-^3F transitions in Al II (Fig. 15) and Si III (Figs. 16 and 17). For doubly excited perturbers located below all or most of the singly excited states of the same symmetry, the interaction range is often shorter than those located in the midst of or above most of the singly excited states except for the $3p^2$ perturber in the Al II $(3snd)^1D$ series. Similar to what was pointed out by Luken and Sinanoglu,[19] we have also found that when there are several singly excited states of the same symmetry located below the doubly excited perturber, special care is needed in the theoretical calculation to determine the interaction strength and its range of influence for that particular symmetry.

Finally, we turn our attention to the question of relativistic interaction. The variation of the J splitting along the Al II ^3F series as illustrated by Weiss[9] clearly suggests that any realistic estimation of the fine-structure splittings will have to include explicitly the configuration mixing in the wave-function calculation. A lowest-order perturbation calculation for the spin-orbit interaction with the multiconfiguration-state wave function employed in the present calculation has shown a correct qualitative feature for the J splittings. Our lowest-order estimation has also shown that contribution from the spin-spin and spin-other-orbit interactions is at least one order of magnitude smaller than the spin-orbit interaction. However, a more reliable calculation will have to include the complete $3p3d$ multiplex (i.e., all $^{1,3}P$, $^{1,3}D$, and $^{1,3}F$ terms) and their neighboring configurations which are strongly mixed with the $3p3d$ configuration. The result of such a calculation will be reported elsewhere.

ACKNOWLEDGMENT

This work is supported by the National Science Foundation under Grant No. PHY84-08333.

[1]U. Fano, Phys. Rev. **124**, 1866 (1961).

[2]See, e.g., G. Bates and P. L. Altick, J. Phys. B **6**, 653 (1973); J. Dubau and J. Wells, *ibid.* **6**, 1452 (1973); P. F. O'Manony and C. H. Greene, Phys. Rev. A **31**, 250 (1985); T. N. Chang, *ibid.* **34**, 4554 (1986).

[3]See, e.g., C. Froese Fischer and J. Hansen, Phys. Rev. A **24**, 631 (1981).

[4]J. Sugar and C. Corliss, J. Phys. Chem. Ref. Data **8**, 865 (1979).

[5]K. T. Lu, J. Opt. Soc. Am. **64**, 706 (1974); M. J. Seaton, Rep. Prog. Phys. **46**, 167 (1983).

[6]T. N. Chang, Phys. Rev. A **34**, 4550 (1986).

[7]T. N. Chang, Phys. Rev. A **36**, 447 (1987).

[8]C. Forese Fischer and M. Godefroid, Phys. Scr. **25**, 394 (1982).

[9]A. W. Weiss, Phys. Rev. A **9**, 1524 (1974).

[10]E. Trefftz and R. N. Zare, J. Quant. Spectrosc. Radiat. Transfer **9**, 643 (1969).

[11]G. A. Victor, R. F. Stewart, and C. Laughlin, Astrophys. J. Suppl. Series **31**, 237 (1976).
[12]R. N. Zare, J. Chem. Phys. **45**, 1966 (1966); **47**, 3561 (1967); A. W. Weiss, *ibid.* **47**, 3573 (1967).
[13]C. Froese Fischer, Phys. Scr. **21**, 466 (1980).
[14]T. N. Chang and Y. S. Kim, Phys. Rev. A **34**, 2609 (1986).
[15]T. N. Chang and U. Fano, Phys. Rev. A **13**, 263 (1976).
[16]C. Bottcher and A. Dalgarno, Proc. R. Soc. London, Ser. A **340**, 187 (1974).
[17]W. C. Martin and R. Zalubas, J. Phys. Chem. Ref. Data **8**, 817 (1979); **12**, 325 (1983).
[18]C. Froese Fischer, Phys. Rev. A **22**, 551 (1980).
[19]W. L. Luken and O. Sinanoglu, Phys. Rev. A **13**, 1293 (1976).